

Experimental study of a horizontal shear-driven liquid film approaching a sharp corner. Critical conditions.

E. Bacharoudis^{*12}, H. Bratec³, L. Keirsbulck¹, J-M. Buchlin², L. Labraga¹

1: Univ. Lille Nord de France, 59000 Lille, France

UVHC, TEMPO, 59313 Valenciennes, France

2: von Karman Institute for Fluid Dynamics, Rhode-St-Genése, Belgium

3: Robert Bosch Produktie N.V., Tienen, Belgium

Abstract

The present work concerns the experimental study of a horizontal liquid film (order of 1-2mm thickness) driven by an external turbulent air flow on a flat plate of low surface energy and its separation due to the presence of a convex sharp corner. The liquid film is formed free on the plate without side wall borders, which would restrict the expansion towards the spanwise direction. Although the slow dependency on time reported during the characterization of the film, the critical conditions, which is the main objective of this study, remain unaffected. The measurements showed that the critical conditions are independent on the variations of the width of the film and depend only on the local film velocity and thickness at the corner. An empirical equation has been proposed to describe the onset of film atomization at the corner. A first attempt to compare the experimental data with models documented in literature shows that further theoretical development is required.

Introduction

Horizontal liquid film flow sheared by an external air flow field and detachment from wall surfaces is a physical phenomenon very common in many engineering applications. The resulting droplets, which usually follow the flow of the external air, can lead to either desirable or detrimental effects. A major cause for the droplet generation can be the inability of the liquid film to negotiate a change in the direction of the initial horizontal flow path.

Liquid films have been studied extensively for decades mainly in two configurations, the horizontal wavy, annular flows and the rectangular channels. The local characteristics and the waves formed on the thin liquid films inside the circular pipes have been investigated by many researchers, selectively reported here Fukano and Ousaka [1], Jayanti et al. [2], Paras and Karabelas [3] and Schubring and Shedd [4]. Less studies have been conducted in rectangular channels, again selectively Cohen and Hanratty [5], Jurman and McCready [6], Wittig et al. [7] and recently, Lan et al [8]. All these studies revealed that mainly three dimensional waves emerge on the interface of the film due to the air-liquid interactions in high external air velocities. The waves affect both the external air and the liquid flow by mainly transmitting energy from the first to the second phase. Concerning the mean characteristics of the liquid film, generally, the film thickness is growing with the rise of the liquid flow rate and is declined with the increase of the air velocity. On the other hand, the liquid flow rate and the air flow above the film result in the increase of the interface velocity. Finally, when the liquid film is not restricted at its sides by the walls of the circular or rectangular channels, see [8], the film width seems to increase with the liquid flow rate and the external air velocity.

The air-liquid interactions resulting in the wavy interface of the horizontal liquid films can provoke the primary atomization and the generation of droplets under certain flow conditions. Several researchers worked experimentally for the detection of the onset of the liquid film entrainment in annular flows, see [9], while less investigated the same phenomenon in horizontal rectangular ducts, ([11], [10]). In addition to the air-liquid interactions, when the liquid film has to deviate its initial flow path due to a geometrical change such as a sharp corner, the droplet generation is pronounced and the flow conditions for the onset of atomization are initiated earlier. Very few researchers have investigated the critical conditions for the onset of liquid atomization around corners and even less have supported their results with experiments. To the knowledge of the authors, three main models based on two general approaches have been proposed in the open literature to predict the onset of atomization around a corner geometry in a co-current, horizontal, air-liquid flow. First, Owen and Ryley [12] proposed a radial stress model based on a force balance in an infinitesimal amount of fluid turning around a bent. In their model, they have taken into account the film inertia, the gravity and the surface tension forces. Very limited and poor experiments have been conducted to validate the model. Second, Maroteaux et al. [13] developed a separation model based on the Rayleigh-Taylor

*Corresponding author: bacharoudis@vki.ac.be

instabilities assuming their rise on the film interface when it turns around the corner. Third, Friedrich et al. [14] suggested a model established on the force balance inside a control volume including the film flowing around the sharp corner. The model incorporates the effect of the angle of the corner. Though they support their model with a significant number of experiments, the experimental method applied to obtain mass measurements and determine the critical conditions is not able to give accurate results very close to the latter. Thus, they concluded that the experimental identification of the critical conditions seems to be quite arbitrary process. A review of the previous models can be found in Wang et al [15] and Wegener et al. [16].

It becomes apparent from the previous works that more experimental evidence is necessary to understand the process of liquid film detachment and determine the critical conditions for the onset of atomization. In this study a horizontal liquid film, free to expand towards the spanwise direction is sheared by a turbulent wall jet developed on the flat plate of an open channel. The liquid film is driven towards the sharp corner of 90° at the edge of the plate. Initially, the characteristics of this type of liquid film flow are presented. The main goal of the study is the experimental investigation of the critical conditions for the onset of liquid atomization at the corner. An empirical model is proposed and the experimental data are compared with the most recent theoretical model in literature. Finally, the influence of the width of the liquid film on the onset of the atomization is discussed.

Experimental facility and methods

The test facility used in this study to investigate the behavior of the shear-driven liquid film and its atomization in a sharp corner is presented in Figure 1. It is consisted mainly on three parts the wind tunnel, the hydraulic circuit and the test section. The wind tunnel is consisted from the parts 1-4 and the hydraulic circuit from the parts 6-10. The test section (5), depicted in detail in Figure 2 is comprised by two plates one horizontal and one vertical forming a sharp corner of 90°. The two plates made by Polycarbonate are restricted by two side walls from PMMA forming a short open channel. The side walls are used to avoid disturbances from the environment, especially at the region where liquid phase detachment occurs. The whole test section is transparent to apply different optical methods for the liquid film study. The test facility has been placed in a large air-conditioned room to avoid perturbations from the jet flow developing at the exit of the wind tunnel. The working fluids were air and distilled water and their properties are shown in Table 1

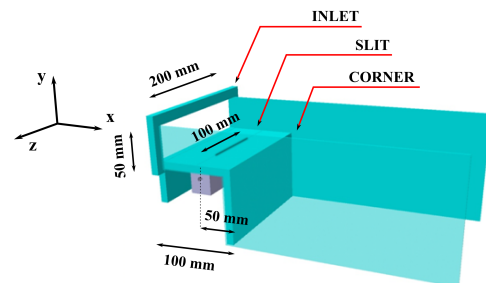
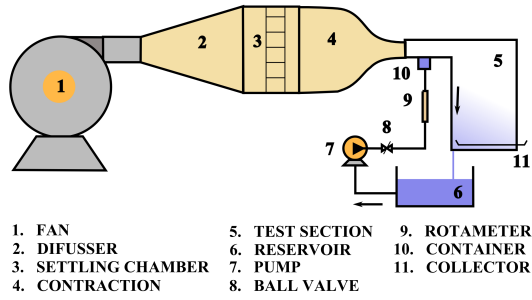


Figure 1. Experimental facility for the study of the shear-driven liquid film on a horizontal plate near a sharp corner.

Figure 2. Detail of the test section.

Distilled water is introduced inside the test section through a long slit of length $w_{slit}=100$ mm and width $h_{slit}=1$ mm with the aid of a small centrifugal pump. The flow rate of the water is measured with a rotameter installed below the test section. The liquid is spread on the horizontal plate and sheared by the turbulent air wall jet developed on the plate towards the sharp corner. There, depending on the flow conditions the liquid film can either flow around or be atomized at the sharp corner. The combination of distilled water with the polycarbonate plate ($\sigma_c=31$ mN/m), which is considered a surface of low energy implies that all the measurement are carried out in the partial wetting regime according to the empirical rules of Zisman reported in [17].

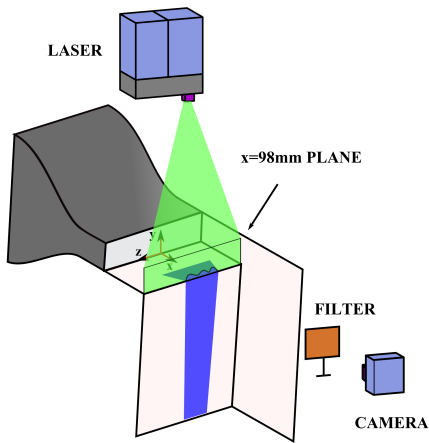
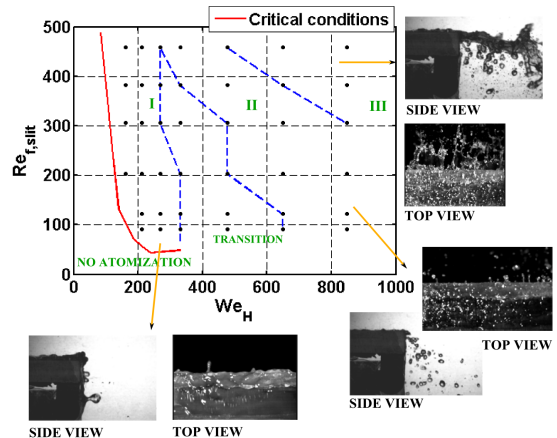
High speed recording has been conducted for the flow visualization campaign. A side camera view with a backward light configuration has been realized to study the shear-driven film and its wavy interface on the plate while a top view with a front light setup has been utilized for the investigation of the liquid film atomization at the corner. The high speed camera works at 1000 fps for all the cases.

Planar Laser Induced Fluorescence (PLIF) has been used to detect the interface and extract the film thickness. Figure 3 shows the plane of measurements of the PLIF setup. Data have been measured at the edge of the corner

Fluid	T [°C]	ρ [kg/m ³]	σ [N/m]	ν [m ² /s]	Contact angle [°]
Distilled water	20	998.2	$72.8 \cdot 10^{-3}$	$1.004 \cdot 10^{-6}$	80.3
Air	20	1.204	-	$15.11 \cdot 10^{-6}$	-

Table 1. Physical properties of working fluids.

to correlate them with the atomization occurring in that region especially for the critical conditions. With the PLIF method the liquid film is visualized and the resulting images are post processed with a Matlab program based on the interface detection through intensity variations. Fluorescein with maximum absorption wavelength at 490 nm and maximum emission wavelength at 518 nm is added in the reservoir as a fluorescent dye in a concentration of 100 mg/l. An Nd:YAG, green (532 nm), single pulse laser illuminates the cross section of the film at the corner with a frequency of 7 Hz. The camera equipped with a lens of 105 mm captures a window of 145 mm length of the liquid film. The spatial resolution of the image is 0.072 mm/pix. A filter is used to suppress the laser light. The images collected are statistically independent and the average film thickness is calculated from the interface detection with a maximum overall uncertainty of 16%.

**Figure 3.** PLIF setup and film thickness plane of measurements.**Figure 4.** Atomization map for horizontal shear-driven liquid film.

Mass measurements have been carried out mainly for the identification of the critical conditions. The method used in this study is the collection of the atomized mass of the film with a small flat collector (11 in Fig. 1) positioned downstream the corner in a distance of 5 mm from the vertical wall of the test section. From the high speed recording when the facility works close to the critical conditions the generated droplets possess enough inertia to be detached from the wall but at the same time their inertia is low to let them escape from the test section. Thus, all the droplets are collected in the plate and are weighed by means of a digital balance with overall uncertainty of ± 0.01 gr. The method becomes inaccurate and stops working for high air velocities. For a pair of flow conditions (air velocity and liquid flow rate), 10 to 20 repetitions of the mass collection are performed and each mass measurement lasts 2 minutes.

Finally, the width of the film has been measured by placing a ruler below the transparent test section and taking pictures with a SLR digital camera from the top. The uncertainty of method is estimated at 1%. From the measured magnitudes of the liquid film flow rate, the mean film thickness and the width, the mean film velocity has been calculated at the corner cross section with an overall uncertainty varying from 4% up to 24%.

Characterization of liquid film

A detailed flow visualization study has been conducted using the high speed recording. The videos have been analyzed and classified as it is depicted in the diagram of the Figure 4. The vertical axis represents the inertia of the film expressed by the liquid Reynolds number ($Re_{f,slit} = \dot{V}_f / (w_{slit} \cdot \nu_f)$), based on the length of the slit

w_{slit} , the liquid flow rate \dot{V}_f and the kinematic viscosity ν_f) while the horizontal axis shows the magnitude of the external air shear expressed by the Weber number ($We_H = \rho_{air} \cdot u_{air}^2 \cdot H / \sigma_f$, based on the air velocity at the center of the potential core of the wall jet developed in the test section u_{air} , the height of the inlet of the test section H , the density of the air ρ_{air} and the surface tension of the film σ_f). Three main regions are distinguished in the area where the film is atomized. Region I (low external shear or high shear and very low film Reynolds number) is characterized by low atomization rates. In this region, regular 3D disturbances are created on the interface of the film moving with it, they reach the corner and turn around forming ligaments, which travel downwards on the vertical wall. Droplets are generated from these ligaments in a long distance from the corner. Increasing the speed of the air flow and the film Reynolds number the atomization regime of the region II occurs. In that regime the free interface of the film is dominated by 3D waves forming a kind of 'cellular' pattern. The atomization mass increases to moderate atomization rates. The waves of the interface form ligaments when encounter the corner and break towards the streamwise direction into droplets due to the strong air flow. For the highest We_H number and film Reynolds number tested here, region III is observed where the atomization is very intense and the wavy liquid film is drifted far from the corner forming a liquid sheet, which breaks into streamwise ligaments and then into small droplets.

A liquid film can obtain different forms when it flows over a horizontal plate without restriction in expanding towards the spanwise direction. Consequently, the behavior of the liquid film and the primary atomization will change for every different film formation. The final form of the film on the plate depends on the initial conditions, the boundary conditions and the ambient conditions of the experiment. In this study, a considerable effort has been made to keep all the conditions constants or at least to minimize their variation. Apart from the sensitivity of the film from all the above conditions, the experiments revealed that there is a weak dependency on the time. Figures 5-13 depict this trend. Though the interest of this study is concentrated on the critical conditions, however, a number of experiments have been conducted in different conditions far from the critical ones to describe the behavior of the liquid film in the open channel configuration of Figure 2.

Three cases have been selected to examine the characteristics of the liquid film on the horizontal plate, the first (Fig.5-7, case 1) and the second case (Fig.8-10, case 2) correspond to conditions relatively far from the critical conditions while the third one (Fig.11-13, case 3) represents the case at the critical conditions. The film at the first row of figures (case 1) has the same liquid Reynolds number with the film at the third row of figures (case 3) but different external We_H number or shear. A comparison of the two cases can reveal the influence of the external air flow field on the film. In a similar manner, the film at the second row of figures (case 2) shares the same We_H number with the third row (case 3) but they have different liquid Reynolds number, thus, the comparison represents the effect of the liquid Reynolds on the film. Initially, it is observed that for constant flow conditions (We_H and $Re_{f,slit}$) far from the critical, the mass that is atomized after the corner (Fig. 5, 8) is continuous but it is reduced with the number of the mass collections or the total time needed the film to flow on the flat surface during the experiment. On the other hand, for the critical conditions the atomization presents an intermittent behavior (Fig. 11). Only 10 acquisitions of the atomized mass, which correspond to a total time of 2 hours have been collected to illustrate the effect of the time on the film. In general, the experiments in this study have been conducted collecting 20 times the atomized mass and in some cases even 60 times to assure that the behavior of the film has been captured.

In order to understand better the atomized mass reduction, the local film width in different positions and the local film thickness at the corner section have been measured for different mass acquisitions. The data reveal that the film (Fig.6, 9) seems to expand slowly but constantly towards the spanwise direction during the experimental procedure. On the other hand the film thickness remains constant with time (Fig.7, 10). The atomized mass reduction seems to occur due to the slow expansion of the film resulting in the reduction of the mean liquid film velocity or the inertia of the film. In conditions far from the critical, which implies high inertia, small reduction of the mean film velocity results in the reduction of the interface velocity and it has a significant impact on the film atomization. The continuous expansion of the film on the plate is believed to arise from the combination of the aerodynamic interactions of the external air flow on the interface creating the disturbance waves, which in their turn cause the deformation of the liquid film with the wetting effects of the partial wetting regime on the contact line at the side of the film. The experiments in this study showed that the atomized mass for conditions far from the critical goes towards zero but never reaches it. Close to the critical conditions, the atomized mass (Fig. 11) seems to remain constant, though the continuous expansion of the liquid film (Fig. 12) remains. The latter signifies that the atomized mass remains unaffected although the film velocity is reduced. It should be reminded that the onset of the film atomization at the corner is primarily a function of the disturbances developed on the film interface. At the critical conditions, the atomization at the corner depicts characteristics of intermittent behavior (Fig 11) as indicated before. Small changes of the mean film velocity shows no significant impact on the wave formation

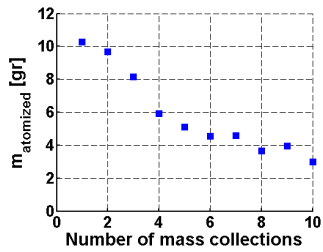


Figure 5. Atomized mass measurements for $We_H = 239$ ($u_{air} = 17 \text{ m/s}$) and $Re_{f,slit} = 92$.

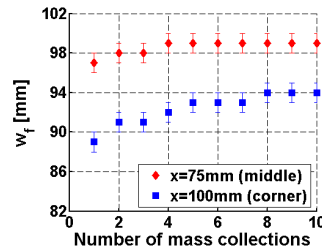


Figure 6. Film width measurements for $We_H = 239$ ($u_{air} = 17 \text{ m/s}$) and $Re_{f,slit} = 92$.

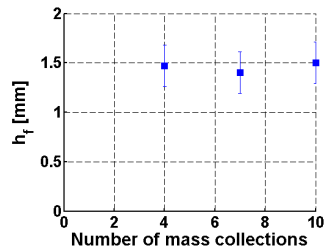


Figure 7. Film thickness measurements for $We_H = 239$ ($u_{air} = 17 \text{ m/s}$) and $Re_{f,slit} = 92$.

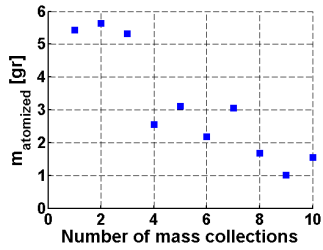


Figure 8. Atomized mass measurements for $We_H = 186$ ($u_{air} = 15 \text{ m/s}$) and $Re_{f,slit} = 130$.

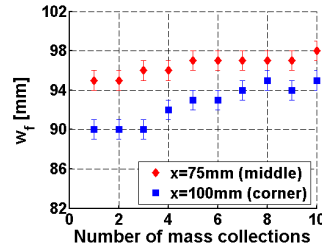


Figure 9. Film width measurements for $We_H = 186$ ($u_{air} = 15 \text{ m/s}$) and $Re_{f,slit} = 130$.

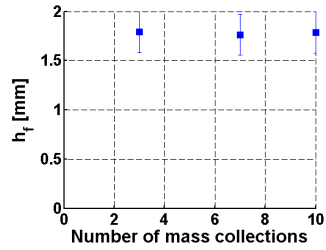


Figure 10. Film thickness measurements for $We_H = 186$ ($u_{air} = 15 \text{ m/s}$) and $Re_{f,slit} = 130$.

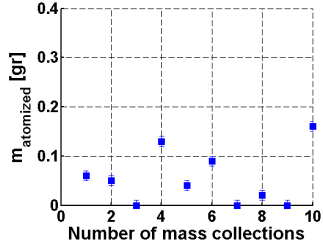


Figure 11. Atomized mass measurements for $We_H = 186$ ($u_{air} = 15 \text{ m/s}$) and $Re_{f,slit} = 92$.

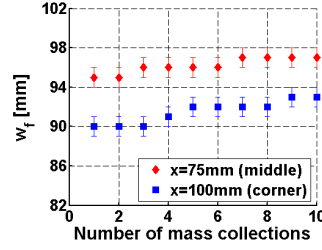


Figure 12. Film width measurements for $We_H = 186$ ($u_{air} = 15 \text{ m/s}$) and $Re_{f,slit} = 92$.

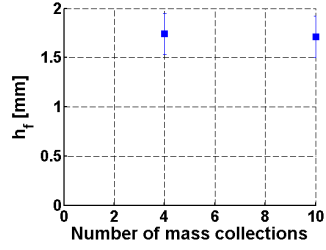


Figure 13. Film thickness measurements for $We_H = 186$ ($u_{air} = 15 \text{ m/s}$) and $Re_{f,slit} = 92$.

and the film atomization in these conditions. The difference observed on the behavior of the atomized mass at the corner under the critical and non-critical conditions permit us to distinguish and detect them.

Finally, the effects of the external air flow field and the film Reynolds number are depicted in Figures 5-13 as mentioned above. Comparing the Figures 11, 8, 5, the atomization at the corner becomes more intense increasing both the external shear and the film Reynolds. The same behavior is observed for the width of the film , Figures 12, 9, 6, rising the air velocity or the film Reynolds number, the film is growing towards the spanwise direction. This trend is in accordance with measurements on film widths reported in literature, see [8] and [14]. On the other hand, the film thickness is reduced increasing the external air velocity, as seen in Fig. 13 and 10 while it remains constant or is decreased raising the liquid Reynolds number as seen in Fig. 13 and 10. The reduction of the mean film thickness with the increase of the liquid flow rate is opposite to what is documented in literature for films in annular flows and rectangular channels. The majority of the films in these studies are restricted to grow in a spanwise direction since either they occupy all the periphery of the pipe or they are limited by side walls of the channel and thus they are developed only to the normal direction.

Critical conditions

This part is mainly focused on the detection of the critical conditions for the onset of the liquid film atomization at the sharp corner and the investigation of the film structure and behavior under these conditions. Responsible parameters for the primary atomization of the film at the corner are considered the external flow and the inertia of

the liquid film generating the wavy interface, which result in the destabilizing centripetal forces at the corner. On the other hand, the surface tension and the viscosity act like stabilizing forces on the liquid film. The gravity do not influence the atomization of the horizontal film.

The primary atomization (or breakup) of the film, which is considered the initial process of the droplet generation from the film taking place during the spray formation at the corner, is influenced significantly by the film width. As shown in the previous part, small variations of the film width could cause considerable changes on the amount of the atomized mass downstream the corner. Approaching the critical conditions, the effect of the film width on the atomization seems to diminish. Since the interest of this study is mainly the onset of the primary breakup, further experiments have been conducted to clarify and confirm that the width do not affect the onset of the film primary atomization. For that reason, the initial length of the slit has been modified and two different liquid films have been developed, one with length of 100 mm and another of 45 mm. The critical conditions are sought in both films and their local characteristics are measured and compared.

The experimental method utilized to determine the critical conditions is the collection and the balance of the atomized mass downstream the corner with a flat collector as shown in Figure 1. The experimental procedure followed to detect the critical conditions is described below. The external air velocity is fixed at a constant value and the film inertia is decreased gradually by reducing the flow rate of the film. Figures 8, 11 depict this procedure. For high film inertia the mass that is atomized is very large, while reducing the film inertia the mass is becoming less. Critical conditions are defined when the atomization of the liquid film exhibits the intermittent behavior shown in Figure 11. Above the critical conditions the liquid film will start to be atomized continuously, while below the critical no mass will be detached from the film and it will flow around the corner.

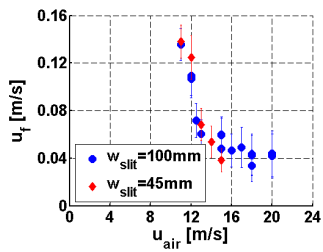


Figure 14. Mean critical film velocity at the corner section.

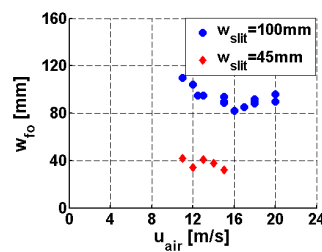


Figure 15. Mean critical film width at the corner section.

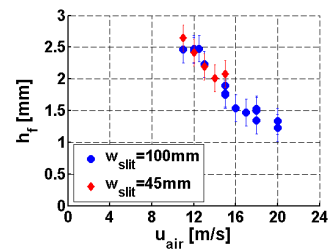


Figure 16. Mean critical film thickness at the corner section.

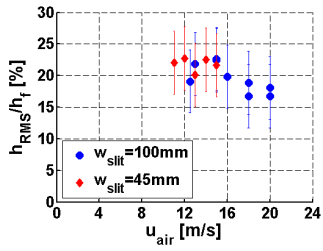


Figure 17. Critical ratio of RMS to mean film thickness measurements at the corner section.

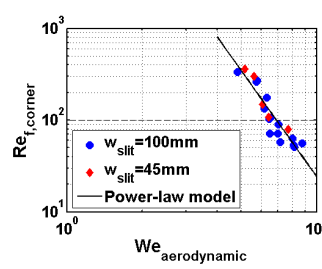


Figure 18. Linear behavior of the critical conditions.

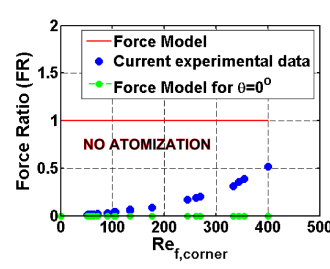


Figure 19. Force Model [14] vs Experimental data.

Using mainly the PLIF method, it was possible to extract useful information concerning the local characteristics of the liquid film. The mean film velocity u_f , the initial film width w_{f0} , the mean film thickness h_f and the dimensionless RMS have been measured at the corner section for the two different films under critical conditions shown in Figures 14-17 respectively. Increasing the external air velocity more energy is added to the film through the shear action, which enhances the inertia of the film and consequently the interface velocity. To maintain the critical conditions, the liquid film has to loose this extra gain of energy. This is achieved by reducing the liquid flow rate in which the film is introduced inside the test section. The liquid flow rate reduction results in the decrease of both the interface velocity and the size of the disturbances formed on the film interface. In terms of average film properties, the result is that the film velocity, width and thickness are reduced to maintain the critical conditions. Figures 14-16 depict this trend. Concerning the effect of the film width at the corner by modifying the length of the slit of the test section, it is interesting to remark that the critical mean film velocity and mean thickness obtain the same values for both slit lengths ($w_{slit}=45$ mm and $w_{slit}=100$ mm). This fact signifies that the onset of the film

atomization will occur when the film velocity and thickness will reach a certain value independently on the film width at the corner. Consequently, although the primary breakup depends on the width of the liquid film at the corner, the onset of the primary breakup is independent on the width. This fact assures that, for the open channel configuration, the slow change of the film width with time, observed in the previous part, will not affect the proper detection of the critical conditions. Finally, the dimensionless RMS comprises a mean to measure the intensity of the fluctuations developed on the interface of the film. Although there is a lot of scattering in the data and the drawing of firm conclusions is not easy, the dimensionless RMS under critical conditions seems to be decreased, Figure 17.

An effort has been made to express all the above results in terms of non-dimensional numbers. Many correlations in literature are expressed as a function of the Weber number and the film Reynolds number based on average values of the film characteristics. The same practice has been followed in this study. The aerodynamic Weber number ($We_{aerodynamic} = \rho_{air} (u_{air} - u_f)^2 h_f / \sigma_f$, based on the difference between the air velocity at the center of the potential core of the wall jet inside the test section and the mean film velocity $u_{air} - u_f$, the mean film thickness h_f , the air density ρ_{air} and the film surface tension σ_f) representing the external shear on the interface and the film Reynolds number ($Re_{f,corner} = u_f h_f / \nu_f$) corresponding to the inertia of the film have been calculated based on the mean film characteristics showed in Figures 14-17. The data have been plotted in a logarithmic graph as shown in Figure 18. The points seem to form a critical line above which atomization occurs while below no mass is detached from the film. The fact that the critical line resembles a straight line implies a power-law relationship between the $We_{aerodynamic}$ and the $Re_{f,corner}$. A linear model has been fitted to the data giving the following empirical correlation:

$$Re_{f,corner} = A \cdot We_{aerodynamic}^n \quad (1)$$

With constants $A=163001$ and $n=-3.83$. The empirical equation 1 describes the onset of the liquid film atomization on a horizontal film approaching a corner of 90° on a low energy surface. It shows that for low external shear (low $We_{aerodynamic}$) the inertia of the liquid film ($Re_{f,corner}$) has to be increased significantly to maintain the critical conditions while for high shear the film inertia has to become very small.

A first attempt to compare the existing experimental results with the results from the literature has been performed. Unfortunately, no experimental data have been found in the open literature concerning the onset of film atomization in a corner of 90° at the edge of a horizontal flat surface. Moreover, the analytical and empirical correlations describing the critical conditions for liquid entrainment concern mainly the annular flows developed in circular pipes. In regard to the flow in rectangular channels, which looks closer to this study, the analytical force model of Friedrich et al. [14] seems suitable for direct comparison with the experimental results. According to that force model a balance among the forces acting on the film at the corner is carried out. Three forces have been captured the film inertia, the surface tension and the gravity. The effect of the corner angle is also included in the correlation. The external air flow field is considered to impact the separation process only through its effect on the film inertia. A force ratio among the forces, which initiate the film separation to the forces resisting the film detachment has been developed. The equation is given below:

$$\text{Force Ratio} = \frac{\rho_f u_f^2 h_f \sin\theta}{\sigma \sin\theta + \sigma + \rho_f g h_f L_b \cos\theta} \quad (2)$$

where $L_b = 0.0388 h_f^{0.5} Re_f^{0.6} We_{rel}^{-0.5}$ given by Arai and Hashimoto [18], $Re_f = h_f u_f \rho_f / \mu_f$ and $We_{rel} = h_f \rho (U_g - u_f)^2 / 2\sigma$. Moreover, u_f is the mean film velocity at the corner, h_f is the mean film thickness at the corner, θ is the corner angle, ρ_f is the density of the film, ρ is the air density and σ the film surface tension. The critical conditions for atomization have been considered when this ratio becomes equal to 1, which implies that the destabilizing forces balance the stabilizing forces on the film. Values below 1 would signify no atomization and values above 1 would imply atomization.

To compare our experimental results with the model, the measurements of the mean local characteristics of the film at the corner section have been introduced inside the equation 2. Since all the experimental results presented here concern the critical conditions, the analytical correlation is expected to give 1 for all the points. Figure 19 depicts the comparison between the force model and the current experimental data. For different critical Re_f the force ratio has been plotted. The force model did not give 1 for the experimental results but a lower value especially when the film inertia is reduced. The model suggests that the film atomization at the sharp corner of 90° has not started since the experimental data correspond to a ratio below 1, although according to the experiment the data

represent the critical conditions. The force model seems to overpredict the onset of the film atomization comparing to these experimental results. The discrepancy is believed to be due to the fact that the model is developed based on the average properties of the liquid film, while the flow visualization study depicts that the atomization at the corner is strongly related to the characteristics of the waves formed on the film interface. Maybe a more appropriate modeling of the phenomenon would include the effect of the wave characteristics. Furthermore, a simple observation on the analytical force model reveals that the case of the film atomization on a flat plate or a corner of angle 0° is not modeled at all. The result coming out from the equation 2 and plotted in Figure 19 is always zero for any flow condition, which implies that on a flat plate there will never happen film atomization according to the force model, which of course is in contrast to the experimental evidence. In that limiting case of the translation of the film (no rotation), the main mechanism of droplet removal is the interaction of the 3D waves on the interface (Kelvin-Helmholtz instabilities) with the air flow above the film. The comparison of the current experiments with the model from the literature suggests that further work has to be done in both experimental and theoretical direction to model more precisely the onset of liquid film separation from a corner geometry.

Conclusions

The primary atomization of a liquid film free to expand towards the spanwise direction on a flat plate of low energy exhibited two different behaviors. Far above the critical conditions, the atomization is continuous but its rate is slowly reduced due to the slow variation of the width of the liquid film. On the other hand, at the critical conditions, the atomization presents an intermittent behavior and the effect of the width variation stops. The critical conditions for the onset of atomization are independent of the size of the film width and depend only on the disturbances on the film interface. A first comparison of the experimental data under critical conditions with proposed analytical models in literature showed that further theoretical development is required to predict accurately the onset of the critical conditions in a corner geometry.

Acknowledgments

The current work has been supported and financed by Robert Bosch Produktie N.V., Tienen, Belgium.

References

- [1] Fukano I., and Ousaka A., *International Journal of Multiphase Flow* 15:403-420 (1989).
- [2] Jayanti S., Hewitt G.F., White S.P., *International Journal of Multiphase Flow* 16:1097-1116 (1990).
- [3] Paras S.V., and Karabelas A.J., *International Journal of Multiphase Flow* 17(4):439-454 (1991).
- [4] Schubring D., and Shedd T.A., *International Journal of Multiphase Flow* 34:636-646 (2008).
- [5] Cohen L.S., and Hanratty T.J., *Journal of Fluid Mechanics* 31:467-479 (1968).
- [6] Jurman L.A., and McCready M.J., *Physics of Fluids A* 1(3):522-536 (1989).
- [7] Wittig S., Himmelsbach J., Noll B., Feld H.J., and Samenfink W., *Journal of Engineering for Gas Turbines and Power* 114:395-400 (1992).
- [8] Lan H., Friedrich M., Armaly B.F., and Drallmeier J.A., *International Journal of Heat and Fluid Flow* 29:449-459 (2008).
- [9] Nigmatulin R.I., Nigmatulin B.I., Khodzhaev YA. D and Kroshilin V.E., *International Journal of Multiphase Flow* 22(1):19-30 (1996).
- [10] van Rossum J. J., *Chemical Engineering Science* 11:35-52 (1959).
- [11] Woodmansee D.E., and Hanratty T.J., *Chemical Engineering Science* 24:297-307 (1969).
- [12] Owen T., and Ryley D.J., *International Journal of Multiphase Flow* 11(1):51-62 (1985).
- [13] Maroteaux F., Lory D., Le Coz J-F, and Habchi C., *Journal of Fluids Engineering* 124:565-575 (2002).
- [14] Friedrich M.A., Lan H., Drallmeier J.A., and Armaly B.F., *Journal of Fluids Engineering* 130:051301-1:9 (2008).
- [15] Wang Y-P., Thiruvengadam M., Drallmeier J.A., and Armaly B.F., *18th Annual Conference on Liquid Atomization and Spray Systems, Americas*, Irvine, CA, May, 2005.
- [16] Wegener J.L., Friedrich M.A., Lan H., Drallmeier J.A., and Armaly B.F., *21th Annual Conference on Liquid Atomization and Spray Systems, Americas*, Orlando, FL, May, 2008.
- [17] de Gennes P-G, Brochard-Wyart F. and Quéré D., *Capillarity an Wetting Phenomena. Drops, Bubbles, Pearls, Waves*, Springer-Verlag New York Inc., 2004.
- [18] Arai T., and Hashimoto H., *Proceedings of the Third International Conference on Liquid Atomization and Spray Systems*, London, (1985).